**Statistical testing and annotation of gene transcriptomic-neuroimaging associations**

Yongbin Wei[1], Siemon C. de Lange[1], Rory Pijnenburg[1], Lianne H. Scholtens[1], Dirk Jan Ardesch[1], Kyoko Watanabe[1], Danielle Posthuma[1,2], Martijn P. van den Heuvel[1,2*]

[1] Department of Complex Trait Genetics, Center for Neurogenomics and Cognitive Research, Amsterdam Neuroscience, Vrije Universiteit Amsterdam, Amsterdam, The Netherlands

[2] Department of Child and Adolescent Psychiatry and Psychology, Section Complex Trait Genetics, Amsterdam Neuroscience, Vrije Universiteit Medical Center, Amsterdam UMC, Amsterdam, The Netherlands

*** Corresponding Author**

Martijn P. van den Heuvel, Ph.D., W&N B-651, De Boelelaan 1085, Amsterdam, 1081 HV, the Netherlands. E-mail: martijn.vanden.heuvel@vu.nl, Telephone: +31 20 59 83343

**Abstract**

Multiscale integration of neuroimaging and gene transcriptome is becoming a widely used approach for exploring the molecular pathways of brain structure and function, in health and disease. Statistical testing of associations between spatial patterns of imaging-based phenotypic and transcriptomic data is key in these explorations, in particular establishing that observed associations exceed 'chance level' of random, non-specific observations. We discuss options for such statistical evaluations, including commonly applied linear regression, null model based on randomized brain regions that maintain spatial relationships, and null models built upon random effects that occur from other genes. Using examples and simulations of analyses as commonly performed in literature, we explain the caveats of these statistical models and provide guidelines for using proper models to evaluate both spatial and gene specificity. The null models are presented in a web-based application called GAMBA ("Gene Annotation using Macroscale Brain-imaging Association") that is designed for exploring transcriptomic-neuroimaging associations.

Keywords: neuroimaging, gene expression, Allen Brain Atlas, brain disorder, connectome

## Introduction

A fast-growing number of imaging-genetic studies is starting to point out associations between gene transcriptome and macroscale imaging-derived brain phenotypes based on overlapped spatial variations of the two scales of brain organization (Richiardi et al., 2015; Wang et al., 2015a; Krienen et al., 2016; Burt et al., 2018). Whole-brain transcriptome data, such as the extensive Allen Human Brain Atlas (AHBA), serves as an invaluable quantitative reference to assess transcriptomic-neuroimaging associations (Hawrylycz et al., 2012). Regional variation in gene expression across regions in the human brain often appears to run parallel with spatial patterns of brain structural and functional features derived from neuroimaging findings [see for reviews (Fornito et al., 2019; van den Heuvel et al., 2019)].

Early examples of such associations include genes related to oxidative metabolism to display transcriptional profiles in a similar spatial pattern as the degree of inter-module long-distance functional connectivity (FC) (Vertes et al., 2016), supporting the notion that brain hub connectivity is more costly in terms of glucose metabolism (van den Heuvel and Sporns, 2013). Others demonstrate that genes enriched for neuronal and synaptic connectivity show transcriptional profiles that capture the architecture of brain functional networks (Krienen et al., 2016; Romero-Garcia et al., 2018b). Brain transcriptional profiles of risk genes related to mental health disorders, such as schizophrenia (Romme et al., 2017), autism spectrum disorder (Romero-Garcia et al., 2018a), and major depressive disorder (Anderson et al., 2020), tend to display overlapping patterns with disorder-specific brain changes revealed by neuroimaging techniques, and have opened a new window for examining how genetic variants associated with brain disorders may relate to changes in brain structure and function.

With transcriptomic datasets often describing data of ~20,000 genes, proper statistical evaluation of observed overlapping patterns of gene expression and imaging-derived features in the context of effects that would happen at chance level (i.e. reflected by the null model) is important, in particular as expression levels of these ~20,000 genes across brain regions are not independent data points (Fulcher et al., 2020). Here, we discuss and evaluate several commonly used options for such statistical evaluations, including commonly applied linear regression, null models based on random brain regions with spatial relationships maintained, and null models on the basis of effects that occur from random genes. We show and discuss that it is crucial to implement proper null models to evaluate both spatial and gene specificity for observed transcriptomic-neuroimaging associations.

## Results

We deliberate on the need and use of null models by means of discussing the analysis strategy and results of three common examples of transcriptomic-neuroimaging investigations, followed by simulations that assess how different null models serve to identify possibly inflated statistical effects. As for examples of typically examined hypotheses in literature (Wei et al., 2019a; Anderson et al., 2020), we hypothesize that the transcriptional profile of a gene/gene-set of interest (GOI) relates to a brain phenotype, like the spatial pattern of brain atrophy (McColgan et al., 2018) or brain disconnectivity (Romme et al., 2017). We test an hypothesized association between the GOI and the brain phenotypes by examining the correlation between the expression pattern of the GOI across the cortex and the pattern of brain features, e.g. atrophy across the cortex (Figure 1a). We then test the statistical relevance of these associations using different strategies: *i)* by methods that assess spatial specificity (Figure 1b) and *ii)* by methods that assess gene specificity (Figure 1c). We show that statistical evaluations based on null models that maintain spatial relationships and include information from other included genes (i.e. all ~20,000 genes in AHBA, or more specific subsets of genes) are highly advised.

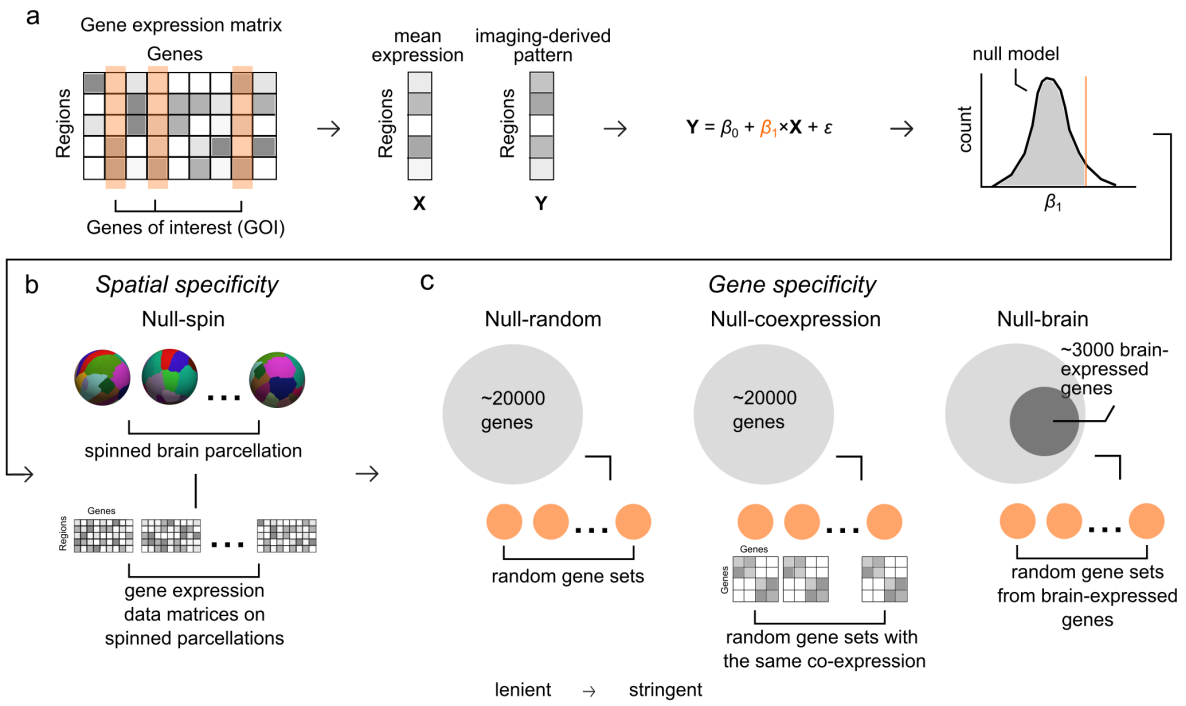


**Figure 1**. *Approaches for statistical testing of overlapping patterns of gene transcription and imaging-derived brain phenotypes.* (a) *Permutation test procedure*. The expression profile (**X**) of a user-defined set of the gene(s) of interest (GOI) is computed. The association between the expression

profile and the imaging-derived pattern (**Y**) is assessed using linear regression. Permutation testing is used to examine whether the observed $\beta_1$ is larger than null distributions of $\beta_1$ derived from null models. Different statistical null models are possible: (b) *Examination of spatial specificity*. The "*null-spin*" model (Alexander-Bloch et al., 2018) is proposed as a method to examine the spatial specificity of the observed associations. Randomized brain parcellations are obtained by spinning the inflated sphere of the real brain parcellation (1000 randomizations). A gene expression data matrix is then rebuilt using these randomized brain parcellations. The rebuilt gene expression data is used to re-evaluate transcriptomic-neuroimaging associations to generate null distributions. (c) *Examination of gene specificity*. Three null models (from more liberal to more stringent) are used to examine the gene specificity. *"Null-random"* model: random genes are selected from all ~20,000 genes included in AHBA. *"Null-coexpression"* model: random genes that conserve the mean co-expression level of the original genes are selected from all ~20,000 genes included in AHBA. *"Null-brain"* model: random genes are selected from a subset of genes (2957 genes) that show up-regulated expression levels in brain tissues in contrast to other body sites.

*Example 1: genes related to cortico-cortical connectivity*

We start by illustrating the procedures for the above mentioned three strategies, re-assessing a commonly examined relationship between the expression of genes important for neuronal connectivity and macroscale connectome organization (Scholtens and van den Heuvel, 2018; van den Heuvel et al., 2019; Wei et al., 2019b). We test this by focusing on 19 genes known to be enriched in supragranular layers of the human cerebral cortex [referred to as human supragranular enriched (HSE) genes], revealed by a previous study that compared gene expression profiles in different cortical layers between mice and humans (Zeng et al., 2012). These HSE genes are suggested to play a role in shaping long-range cortico-cortical connections of layer III pyramidal neurons and as such to show a spatial expression pattern that runs parallel to the organization of brain structural and functional networks (Krienen et al., 2016; Romero-Garcia et al., 2018b). The transcriptional profile of HSE genes is shown in Figure 2a.

*Transcriptomic-neuroimaging overlap: linear regression.* We first examine the spatial expression pattern of HSE genes in the context of macroscale brain connectome properties. Using simple linear regression we indeed (Romero-Garcia et al., 2018b) note that the expression pattern of HSE genes is significantly associated with the pattern of connectivity strength of cortical areas – a measurement describing the extent to which a region is connected to the rest of the brain [standardized beta ($\beta$) = 0.672, $p < 0.001$ for connectivity weighted by the number of streamlines (NOS); $\beta = 0.631$ $p < 0.001$ for connectivity weighted

by streamline density (SD); false discovery rate (FDR) corrected for multiple testing across five connectome-related metrics; Figure 2b,c]. A similar association can be found between the pattern of HSE gene expression and the pattern of nodal strength of the functional connectome (FC; $\beta = 0.442$, $p < 0.001$; FDR corrected; Figure 2b,c), which is fully in line with the notion of a strong correspondence between structural and functional connectivity (Wang et al., 2015b).

*Spatial specificity: null-spin model.* These findings thus confirm a potential association between HSE gene expression and macroscale connectome organization (Krienen et al., 2016; Romero-Garcia et al., 2018b), but it is worth noting that whether such associations are *spatially* specific (i.e. specific to examined brain regions) or *genome-wise* specific (i.e. specific to HSE genes) has to be further tested. To do so, the first consideration is whether such a relationship is spatially specific. As importantly put forward recently (Alexander-Bloch et al., 2018; Fulcher et al., 2020), the commonly used linear regression method assumes no auto-correlation for independent variables, which means no correlation between values (i.e., expression levels) of the same variable [i.e., gene(s)] across different observations (i.e., regions). It is thus crucial to examine whether the observed associations are biased by potentially correlated expressions of neighboring brain regions, i.e. preserving spatial relationships across regions. To this end, an important new null model has been introduced, namely the "null-spin" model (Alexander-Bloch et al., 2018), where transcriptomic samples are assigned to brain regions from randomized parcellations that are obtained by spinning the reconstructed sphere of the real brain parcellation, importantly preserving spatial relationships across brain regions (1,000 randomizations; see Methods, Figure 1b). The rebuilt gene expression data matrices are used to generate a null distribution of $\beta$, which is used to assess whether the original effect goes beyond the null condition. Using the null-spin model, the associations between the expression pattern of HSE genes and the pattern of structural/functional connectivity strength are again found to be significant (NOS: $z = 3.372$, $p < 0.001$; SD: $z = 2.473$, $p = 0.013$; FC: $z = 2.051$, $p = 0.040$; Figure 2d). These effects thus significantly go beyond effects that one can expect using randomized brain regions with the same neighboring relationships, suggesting that the observed associations are specific to the spatial organization of brain regions.

*Gene specificity.* Spatial specificity however does not yet tell us anything about whether the observed effect goes beyond the effect that one could expect from any other set of gene(s). We thus argue that the next important step in the evaluation of the observed association(s) between transcriptomic profile(s) and spatial patterns of the imaging-derived

brain phenotypes is to examine to what extent the computed linear correlations exceed effects that one could also observe when *any* other gene or set of genes would have been chosen, i.e. a set of not-of-interest genes. This follow-up step is not yet commonly made in transcriptomic-neuroimaging investigations. We particularly note that this step is of particular importance as multiple examinations have pointed out general (i.e. global) posterior-anterior gradients of expression levels across brain areas (McColgan et al., 2018; Vogel et al., 2020), effects that may more reflect spatial patterns general to genes expressed in the brain, rather than reflecting patterns unique to the GOI. With transcriptomic datasets such as AHBA generally containing data of ~20,000 genes, it is important to go beyond statistical testing of a spatial association between the expression pattern of a GOI and the cortical pattern of a phenotype of interest.

*Null-random model*. For this purpose, we employ permutations to generate null distributions of effect sizes, $\beta$, based on gene expression profiles of same-sized gene sets randomly selected from all genes (by default 10,000 permutations are used). We refer to this commonly used null model (Romme et al., 2017; Fulcher et al., 2020) as the "null-random" model (Figure 1c). When the original $\beta$ significantly exceeds this null model, it indicates the observed association cannot be found for all genes, but is unique for the GOI. For our HSE example, we show that the observed effect sizes for associations between HSE genes and nodal strength of structural and functional connectivity are significantly larger than effect sizes of random genes (NOS: $z = 5.810$, $p < 0.001$; SD: $z = 4.660$, $p < 0.001$; FC: $z = 3.124$, $p = 0.003$; Figure 2d).

*Null-coexpression model.* We (Wei et al., 2019a) and others (Fulcher et al., 2020) have, however, further noted that when a set of genes (instead of a single gene) is examined, the co-expression level within the set of genes can influence the association between the mean gene expression profile and the imaging-derived phenotype. For example, if a GOI contains a large subset of strongly co-expressed genes, this subset of genes would largely determine the mean gene expression profile and hence the correlation between the mean gene expression profile and phenotypes, something that is not taken into account in the null-random model, which is a random mixture of genes (Fulcher et al., 2020). Therefore, we argue that it would be more informative to further include a null model for stricter statistical evaluation, comparing the observed effect size to the null distribution of effect sizes yielded by random genes conserving the same level of co-expression as the input GOI (referred to as "null-coexpression"; Figure 1c). For our HSE example, we use simulated annealing to look for random genes with the mean co-expression levels converging to those of HSE genes (see

Methods). Application of this null model still shows significant associations between HSE gene expression and connectivity strength (NOS: $z = 5.690$, $p < 0.001$; SD: $z = 4.640$, $p < 0.001$; FC: $z = 3.114$, $p = 0.002$; Figure 2d).

*Null-brain model.* We anticipate that the strongest usability of transcriptomic-neuroimaging examinations is to link brain transcriptomic data (like AHBA) to brain phenotypes (like MRI measurements). Most of such examinations will thus be centered on testing a GOI pre-selected based on the findings from previous studies, e.g. GWAS of a disease phenotype like schizophrenia (Schizophrenia Working Group of the Psychiatric Genomics, Consortium, 2014) or Alzheimer's disease (Jansen et al., 2019), a specific pathway related to neuronal properties (Kepecs and Fishell, 2014) as in our first HSE example, genetic variants related to brain volume (Jansen et al., 2020), etcetera. The result of such pre-selected GOI is that most of them will likely be related to processes related to the brain, and as such reflect genes likely over-expressed in brain tissue. As a consequence, we argue that in these cases a null condition generated by randomly selecting genes from the total set of ~20,000 genes (including genes related to all body processes, certainly not only to the brain) is not fair and too liberal, as the null-condition will include a body of background genes not, or less, expressed in brain tissue. Including such genes into the null-condition will lead to a too liberal null-distribution of effects and with that an overestimation of the original effect (de Leeuw et al., 2018).

To avoid this, we advise using a null model that tests whether the observed effect size is larger than the null distribution of effect sizes based on background genes that are particularly expressed in brain tissue. We refer to this null model as "null-brain" (Figure 1c) (Wei et al., 2019a), with random genes now selected from the pool of genes that are significantly more expressed in brain tissues in contrast to other body sites. This selection can for example be made according to the GTEx database (Consortium, G. TEx, 2015), containing gene expression data of all sorts of body tissues, including the brain (2957 brain-expressed genes selected by $q < 0.05$, FDR correction, one-sided two-sample *t*-test). In our example, using this stricter null model now confirms significant associations between HSE genes and connectome metrics (NOS: $z = 4.445$, $p < 0.001$; SD: $z = 4.283$, $p < 0.001$; FC: $z = 2.698$, $p = 0.007$; Figure 2d).

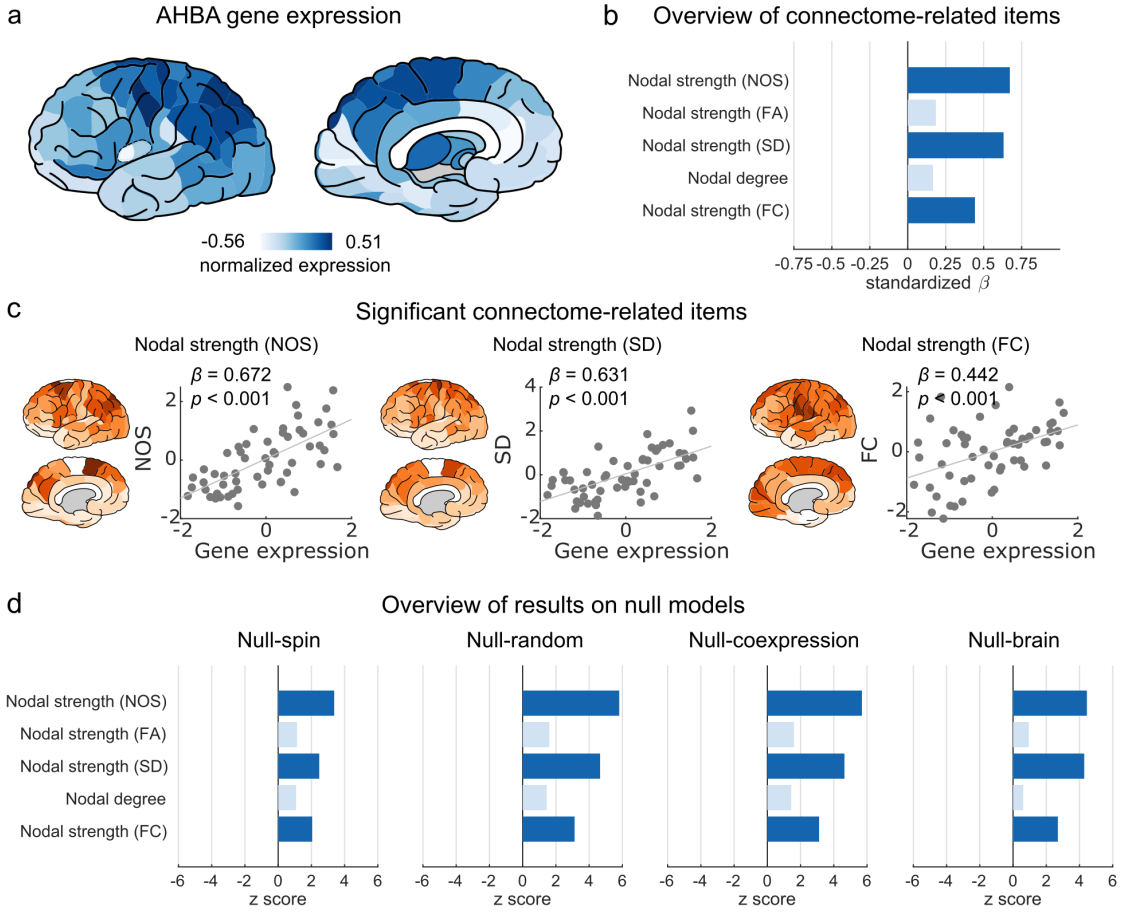


**Figure 2.** *HSE gene expression and macroscale connectome properties.* (a) Brain plots of normalized gene expression levels of HSE genes. (b) Overview of linear regression results between HSE gene expression profile and five imaging-derived connectome properties included in GAMBA. Dark blue indicates significant ($q$ < 0.05, FDR corrected across 5 connectome traits). (c) Scatter plots for significant correlations between HSE gene expression and nodal strength of the structural (NOS-weighted, $\beta$ = 0.672 and SD-weighted, $\beta$ = 0.631) and functional connectome ($\beta$ = 0.442). (d) Permutation testing results showing whether the observed effect size ($\beta$ in panel b) is significantly beyond four distinct null distributions of effect sizes for null-spin, null-random, null-coexpression, and null-brain models. Dark blue indicates $p$ < 0.05 (two-tailed $z$-test).

*Example 2: Alzheimer's disease risk gene APOE*

Our HSE example shows a case in which the main hypothesized effect survived all different statistical evaluations, from liberal linear regression to more strict (i.e. providing needed spatial and gene specificity) null-coexpression and null-brain models, showing both spatial and gene specificity. In a second example, we show that this however is not always the case, with the use of a (too) liberal statistical test not testing for spatial and/or gene specificity, potentially leading to the report of false-positive associations. Here, we zoom in on

transcriptomic brain patterns of disease-related pathology, another major topic of combined transcriptomic-neuroimaging studies (Romme et al., 2017; McColgan et al., 2018; Freeze et al., 2019). We examine the Apolipoprotein E (*APOE*) gene, widely indicated as a risk gene for Alzheimer's disease (AD) (Liu et al., 2013). We hypothesize that the cortical gene expression of *APOE* is related to the cortical alterations revealed in patients with AD or other types of dementia (Grothe et al., 2018), and that correlation analysis between transcriptomic and neuroimaging data may provide evidence for such a relationship.

We again start by examining potential overlap in the transcriptional profile of our gene of interest, here *APOE* (Figure 3a), and a neuroimaging phenotype of interest, here cortical atrophy patterns of 22 brain diseases, including AD, dementia, and others as reported by meta-analyses of the BrainMap voxel-based morphometry (VBM) studies (see Methods). Linear regression analysis first reveals that the pattern of *APOE* gene expression is significantly associated with results of VBM studies reporting on atrophy of brain regions in *i)* dementia ($\beta = 0.653$, $p < 0.001$), *ii)* AD ($\beta = 0.631$, $p < 0.001$), *iii)* semantic dementia ($\beta = 0.620$, $p < 0.001$) and *iv)* frontotemporal dementia ($\beta = 0.505$, $p = 0.001$; FDR corrected for multiple testing across 22 diseases; Fig 3b,c). This seems to nicely confirm our hypothesis. Exploratory analysis seems to reveal additional associations between *APOE* expression and the atrophy pattern of *v)* attention deficit hyperactivity disorder (ADHD) which has been hypothesized as a risk factor of dementia pathology (Callahan et al., 2017) ($\beta = 0.349$, $p = 0.008$) and vi) bipolar disorder ($\beta = 0.335$, $p = 0.010$; Figure 3b).

As a subsequent step, we use the null-spin model to examine the *spatial specificity* for the above-mentioned associations between *APOE* transcriptional profile and atrophy patterns in the observed brain diseases. Using this null model reveals significant associations of *APOE*'s expression with brain atrophy in 5 out of the 6 diseases listed above, including dementia ($z = 3.518$, $p < 0.001$), AD ($z = 3.336$, $p < 0.001$), frontotemporal dementia ($z = 3.331$, $p < 0.001$), semantic dementia ($z = 2.762$, $p = 0.006$), and bipolar disorder ($z = 2.143$, $p = 0.032$; Figure 3d). These findings show encouraging effects that favors a relationship between the transcriptional profile of *APOE* and patterns of cortical atrophy related to dementia.

However, when we evaluate whether the observed associations between *APOE* transcriptional profile and disease-related atrophy patterns exceed effects that one could also observe by chance for *any* other set of genes, these effects diminish. Among the six diseases revealed in linear regression analysis, only the effects for semantic dementia ($z = 2.057$, $p = 0.040$) and dementia ($z = 2.001$, $p = 0.045$) remain significant when using the null-random

model (i.e., random genes selected among all genes); the other effects no longer show significance (AD: $z$ = 1.938, $p$ = 0.053, frontotemporal dementia: z = 1.928, $p$ = 0.054; bipolar disorder: $z$ = 1.271, $p$ = 0.204). Moreover, using the stricter null-brain model (i.e. zooming in on genes expressed in brain tissue) none of the above effects remain significant (all $p$ > 0.05). This suggests that the initially found association between the expression pattern of *APOE* and the atrophy patterns of e.g. AD, frontotemporal and semantic dementia, do not exceed effects that can be generally observed when any other (random) gene expressed in brain tissue would have been selected.

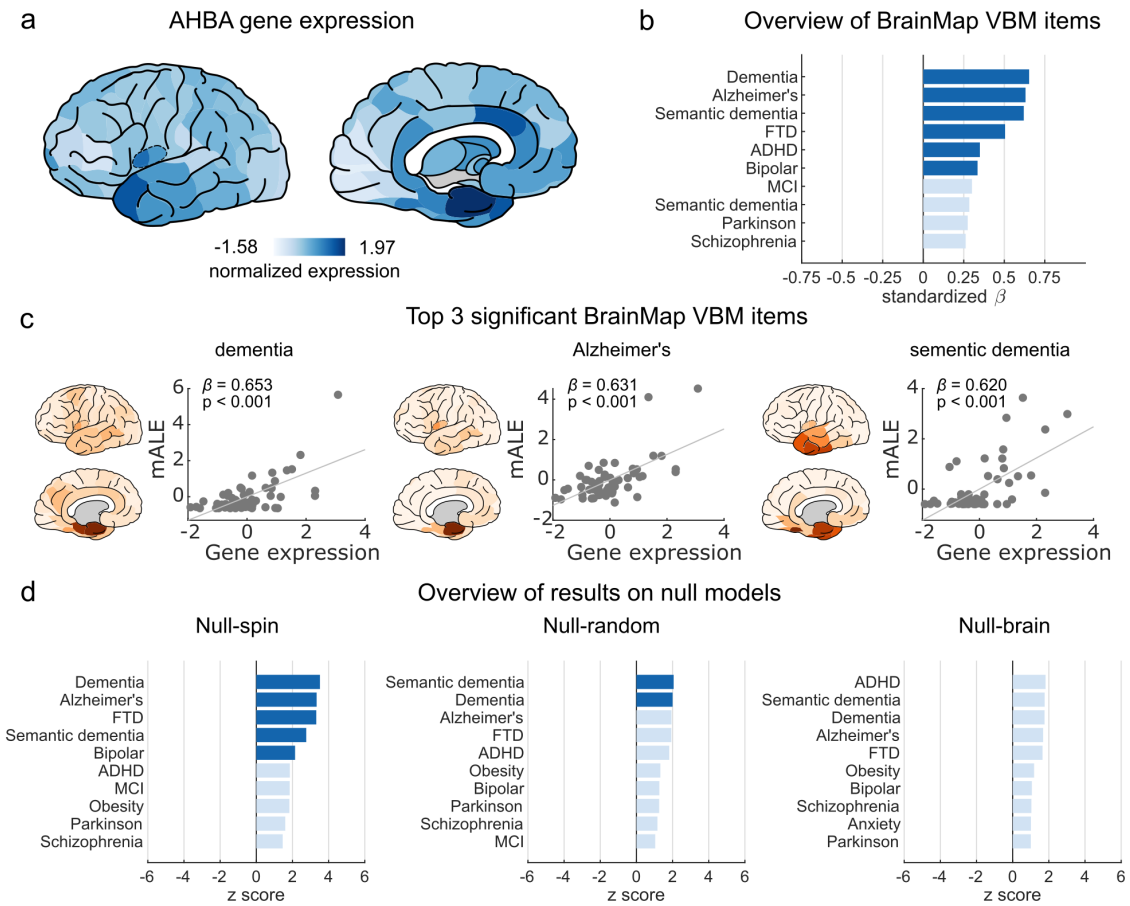


**Figure 3**. *APOE gene expression and atrophy in brain diseases.* (a) Brain plots of normalized gene expression levels of *APOE*. (b) Overview of linear regression results, showing the top 10 associations between *APOE* gene expression profile and the BrainMap voxel-based morphometry (VBM)-derived atrophy patterns included in GAMBA. Dark blue indicates significant ($q$ < 0.05, FDR corrected across 22 brain diseases included in GAMBA). (c) Top 3 significant correlations between *APOE* gene expression and VBM changes in dementia ($\beta$ = 0.653), Alzheimer's ($\beta$ = 0.631), semantic dementia ($\beta$ = 0.620). (d) Permutation testing results showing whether the observed effect size ($\beta$ in panel c) is

significantly beyond three distinct null distributions of effect sizes for null-spin, null-random, and null-brain models. Dark blue indicates $p < 0.05$ (two-tailed $z$-test).

*Example 3: Application to autism spectrum disorder risk genes*

We further demonstrate the importance of null-model selection to avoid an over-interpretation of found associations in a third example. We examine gene expressions of 25 risk genes of autism spectrum disorder (ASD, 24 of which are present in AHBA) obtained from a recent meta-analysis of genome-wide association studies on a total of 18,381 ASD cases and 27,969 controls (Grove et al., 2019). Again, in a first examination, we compute the correlation between the expression pattern of ASD genes (Figure 4a) and functional alterations in brain diseases derived from BrainMap data (Fox and Lancaster, 2002; Fox et al., 2005; Laird et al., 2005), which reveals an interesting association with Asperger's syndrome ($\beta = 0.284$, $p = 0.032$, not corrected) (Figure 4b) -- a major diagnosis of ASD with difficulties in social interaction and nonverbal communication. The subsequent analysis further suggests that this effect for ASD genes is spatially specific as shown by the application of the null-spin model ($z = 1.991$, $p = 0.047$). However, using null models to examine gene specificity does not show any significant result (null-random: $z = 1.217$, $p = 0.223$; null-coexpression: $z = 1.354$, $p = 0.076$; null-brain: $z = 1.246$, $p = 0.213$; Figure 4c). This simple example shows that even when an expected association is observed that fits with current theories of brain (dis)organization and (dis)connectivity, these effects may be overestimated, with other sets of genes (in this case, random subsets of genes generally expressed in brain tissue) showing similar expression patterns. We thus again argue that the selection of a proper null model matching one's research question is of importance in linking brain expression data to neuroimaging phenotypes.

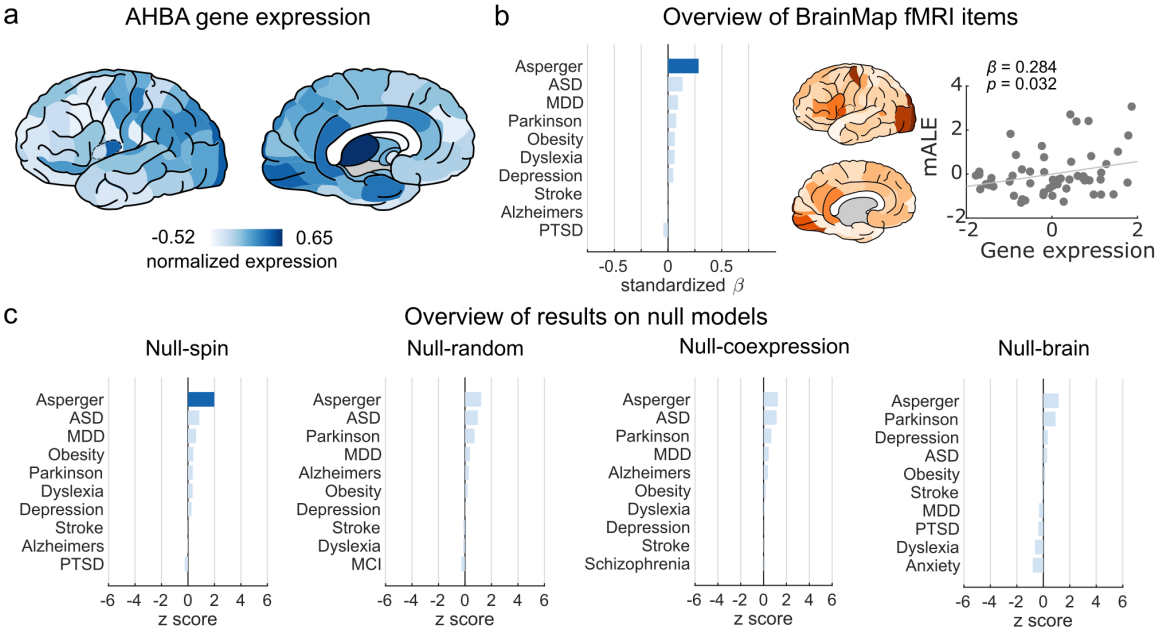


**Figure 4**. *ASD gene expressions and functional alterations in brain diseases.* (a) Brain plots of *z*-scores, showing to what extent the expression level of 24 ASD genes is higher than the average gene expression. Yellow circles indicate $p < 0.05$. (b) Overview of linear regression results, showing the top 10 associations between *ASD* gene expression profile and the disease-related BrainMap functional alterations included in GAMBA, with Asperger's syndrome showing the highest correlation ($\beta$ = 0.284, $p$ = 0.032, not corrected). (c) Permutation testing results showing whether the observed effect size ($\beta$ in panel c) is significantly beyond four distinct null distributions of effect sizes for null-spin, null-random, null-coexpression, and null-brain models. Dark blue indicates $p < 0.05$ (two-tailed *z*-test).

**Table 1**. Summary of examples statistically testing associations between spatial patterns of gene expression and imaging-derived brain phenotypic patterns

| Examples | Linear regression (standardized $\beta$) | Spatial specificity | Gene specificity | | |
|---|---|---|---|---|---|
| | | null-spin (*z*-score) | null-random (*z*-score) | null-coexpression (*z*-score) | null-brain (*z*-score) |
| HSE genes & connectivity strength (NOS) | **0.672** | **3.372** | **5.810** | **5.690** | **4.445** |
| *APOE* & VBM changes in dementia | **0.653** | **3.518** | **2.001** | NA | 1.744 |
| ASD genes & fMRI changes in Asperger's syndrome | **0.284** | **1.991** | 1.217 | 1.354 | 1.246 |

**bold**: significant

*Quantitative evaluation of null models*

*Brain phenotypes*. We provided three simple examples of analyses and results of commonly performed transcriptomic-neuroimaging studies in recent literature (Fornito et al., 2019). To provide deeper insight into the comparison of the different null-model strategies and their effect on reporting potential false-positive results, we continue by simulating the outcome of the discussed statistical evaluation approaches for a wide range of real brain phenotypes and artificial gradients. To this end, we build a full outcome-space of all associations between single-gene expression profiles in AHBA (20,949 in total) and 384 imaging-derived brain phenotypes taken from multiple sources such as NeuroSynth (Yarkoni et al., 2011), BrainMap (Fox and Lancaster, 2002; Fox et al., 2005; Laird et al., 2005) and Cognitive Ontology (Yeo et al., 2016) (see methods). Among all these gene × brain phenotype (20,949 × 384) associations, the linear model indicates 960,963 (11.85%) of these associations as significant ($p < 0.05$, uncorrected), with 208,190 (2.57%) reaching FDR and 56,259 (0.69%) reaching Bonferroni correction with $\alpha$ level < 0.05 (corrected for 384 tests of all brain phenotypes per gene). We then implement null models to examine the spatial/gene specificity for the potential significant associations. Only FDR-corrected results are reported in the following paragraphs for the sake of simplicity. Uncorrected and Bonferroni-corrected results are tabulated in Table 2.

Using the null-spin model to assess spatial specificity shows that 26,273 out of the 208,190 associations reported in linear regression remain significant ($p < 0.05$, null-spin; Supplementary Figure S1). This finding indicates that a large proportion of transcriptomic-neuroimaging associations revealed in linear regression (87%) are probably overestimated due to simple dependencies of gene expressions among neighboring brain regions and are thus likely to be false-positive findings. This is in line with what was recently reported by Fulcher and colleagues (Fulcher et al., 2020).

When we then further implement the null-random and null-brain models (null-coexpression not applicable for single-gene analysis) to examine gene specificity of the reported transcriptomic-neuroimaging associations, we find that only 15,297 out of these 26,273 reported associations surviving the null-spin model remain further significant using the null-random model ($p < 0.05$, null-random & null-spin). This result suggests that even among spatially specific associations, there is still a considerable proportion of associations (42%) that are commonly found for a wide range of genes and do not show gene specificity. These effects likely reflect effects that are not (highly) specific to the GOI. Using the more stringent null-brain model (i.e. selecting the null-distribution from the more focussed subset

of brain genes) shows that only 9,802 associations out of the 26,273 associations surviving the null-spin model remain significant ($p < 0.05$, null-brain & null-spin; Supplementary Figure S1). Importantly, compared to results of the null-random model, 5,495 (36%) associations do not reach significance using the null-brain model. These associations are thus argued to be effects that can be observed for general brain-expressed genes and likely less informative in terms of brain-related functions.

Similar results are noted when we apply null models the other way around, namely, first applying the null-brain model and then the null-spin model. Doing so, we identify 67,181 gene-set specific associations ($p < 0.05$, null-brain) of which only 15% (9,802) are spatially specific ($p < 0.05$, null-spin & null-brain; Supplementary Figure S1), indicating that gene and spatial specificity are not mutually inclusive.

Similar findings are also observed for gene sets of more than one gene by examining transcriptomic-neuroimaging associations for gene sets curated in the Gene Ontology (GO) database (http://geneontology.org) (see for details in the Supplementary Results).

**Table 2**. Summary of all potential associations between spatial patterns of single-gene expression and 384 imaging-derived brain phenotypic patterns

| Methods | Number of significant associations ($\alpha$<0.05) | | |
|---|---|---|---|
| | uncorrected | FDR-corrected | Bonferroni-corrected |
| LR | 960,963 | 20,8190 | 56,259 |
| LR & N-spin | 84,149 | 26,273 | 8,142 |
| LR & N-spin & N-rand | 26,786 | 15,297 | 7,610 |
| LR & N-spin & N-brain | 19,551 | 9,802 | 6,294 |

LR: Linear Regression; N-spin: Null-spin model; N-rand: Null-random model; N-brain: Null-brain model

*Simulated phenotypes*. In the previous paragraphs we demonstrate the need of examining spatial and gene specificity of observed transcriptomic-neuroimaging associations. We continue by showing this to be particularly important when testing phenotypes with spatial patterns similar to global posterior-anterior or inferior-superior gradients (McColgan et al., 2018; Vogel et al., 2020). To elaborate this point, we simulate spatial maps of seven phenotypes that simply follow global spatial gradients across the brain, from posterior to anterior, from inferior to superior, and from medial to lateral, together with the four combinations of these gradients (Supplementary Figure S2). We then examine all associations between single-gene expression profiles in AHBA and the simulated phenotypes. Among all

these possible associations (20,949 × 7), we can find 23,723 (16%) significant associations between single-gene transcriptional profiles and simulated phenotypic profiles (linear regression: $q < 0.05$, FDR corrected; corrected for 7 tests of all simulated phenotypes per gene).

These results are suggestive of a large set of genes with expression profiles that follow general spatial gradients of the brain, and thus show a rather non-specific spatial pattern that is shared with a wide range of other genes. Application of the null-spin model to these associations shows that only 3,305 out of the observed 23,723 associations (14%) remain significant, suggesting that most of the effects resulted from linear regression are inflated due to the strong spatial dependency of neighboring brain regions and can be filtered out by the null-spin model. Among those 3,305 spatial-specific associations, only 974 (29%) further remain significant when we additionally apply the null-random model. An even smaller number of significant associations can be observed (626; 19%) when we use the stricter null-brain model (Supplementary Figure S1).

These simulations show that only 3% (626 out of 23,723) of the associations between the single-gene transcriptional profile and spatial gradients revealed in linear regression can be labeled as both spatially specific and gene-set specific; 97% of the initially found FDR-corrected effects do not survive additional statistical testing (11.3% only spatially specific, 11.7% only gene-specific). Most correlations reported by using simple linear regression thus tend to reflect an effect caused by trivial spatial associations between neighboring brain regions and/or effects that could similarly be found for many of the other genes in the total dataset as they show a common pattern across brain regions (Fulcher et al., 2020).

**Table 3**. Summary of all potential associations between spatial patterns of single-gene expression and 7 simulated brain phenotypes that represent global spatial gradients

| Methods | Number of significant associations ($\alpha$<0.05) | | |
|---|---|---|---|
| | uncorrected | FDR-corrected | Bonferroni-corrected |
| LR | 33,335 | 23,723 | 18,336 |
| LR & N-spin | 3,880 | 3,305 | 3,175 |
| LR & N-spin & N-rand | 1,003 | 974 | 967 |
| LR & N-spin & N-brain | 647 | 626 | 620 |

LR: Linear Regression; N-spin: Null-spin model; N-rand: Null-random model; N-brain: Null-brain model.

*GAMBA platform*

To facilitate examinations on transcriptomic-neuroimaging associations and test results across different null models, we present a simple web-based application, GAMBA (short for Gene Annotation using Macroscale Brain-imaging Association). Within the tool, expression profiles of input GOIs can be linked to imaging-derived brain traits from nine categories (Figure 5). Imaging-derived phenotypes included already in the tool cover the spatial patterns of a) resting-state functional networks (Yeo et al., 2011), b) brain cognitive components (Yeo et al., 2016), c) regional metrics of the brain structural and functional connectome, d) measurements of the cortical oxygen and glucose metabolism (Vaishnavi et al., 2010), e) human surface area expansion compared to the chimpanzee (Wei et al., 2019a), f) brain volume alterations across twenty-two disorders (Fox and Lancaster, 2002; Fox et al., 2005; Laird et al., 2005), g) brain functional changes in sixteen disorders (Fox and Lancaster, 2002; Fox et al., 2005; Laird et al., 2005), h) cortical patterns of brain (dis)connectivity across nine psychiatric and neurological disorders (de Lange et al., 2019), i) brain functional correlates of 292 terms in relation to cognitive states and brain disorders, as described in the NeuroSynth database (Yarkoni et al., 2011). Details on the datasets and statistical analyses are described in the Supplementary Methods. Besides these pre-set neuroimaging phenotypes the user can upload his/her neuroimaging data for cross-reference with the transcriptomic data. GAMBA is available online at http://dutchconnectomelab.nl/GAMBA/.

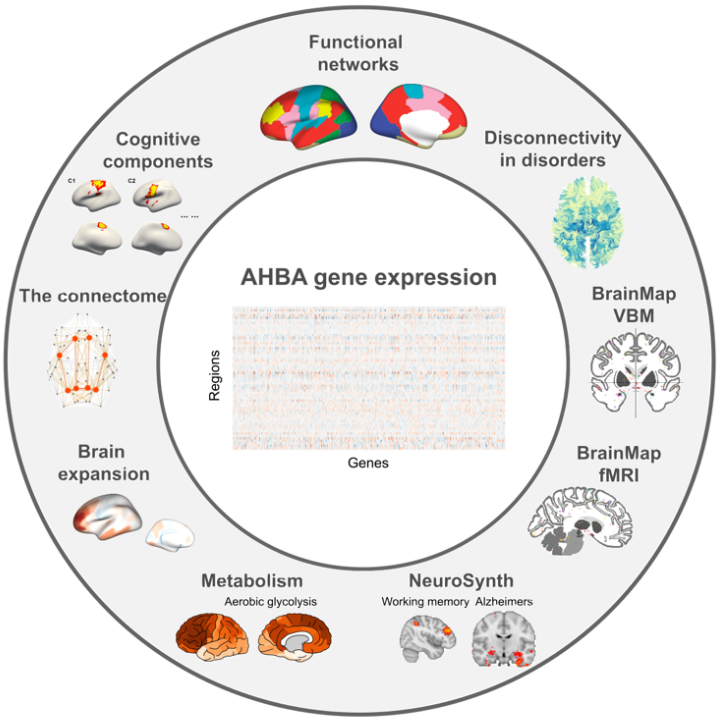

**Figure 5**. *An overview of the preset imaging-derived phenotypes included in GAMBA*. Brain gene expressions are extracted from the Allen Human Brain Atlas (AHBA) and are cross-referenced to distinct imaging-derived brain phenotypes. Brain phenotypes include (counterclockwise) functional networks, cognitive components, metrics of the connectome, evolutionary brain expression, and metabolic measurements in the healthy, and disconnectivity, structural and functional alterations in the diseased brain, as well as terms in NeuroSynth (see Methods).

## Discussion

We evaluate and discuss the importance of selecting a null-condition when performing a transcriptomic-neuroimaging study. We show the usability of several commonly applied statistical methods, including single linear regression and the null-spin model to provide spatial specificity, and three other null models based on null-distributions derived from randomly selected genes to provide additional gene specificity. We recommend the use of appropriate null models when examining overlapped spatial patterns of transcriptomic profiles and imaging-derived phenotypes, providing information on both spatial and gene specificity based on the research question asked.

The three examples we present obviously do not cover all types of examinations one can perform by combining transcriptomic and neuroimaging data. They do however illustrate some of the caveats and limitations of cross-linking cortical patterns of transcription and neuroimaging features and recommend the use of additional statistical analyses. Our first example illustrates that transcriptomic-neuroimaging associations can include effects that are both spatial- and gene-specific. We show that the cortical transcriptional profile of HSE genes runs parallel to spatial patterns of macroscale brain traits. Effects go beyond both general spatial and random-geneset effects that could be expected based on chance level alone and thus highlight an interesting relationship between expression patterns of genes related to neuronal and macroscale connectivity (Zeng et al., 2012; Krienen et al., 2016; Romero-Garcia et al., 2018b).

A different conclusion should however be made when examining *APOE* and the set of ASD genes, with the two examples underscoring the importance of proper statistical testing. The expression pattern of *APOE* across cortical areas seems to show, at first glance, a sensible and significant correlation with reported patterns of structural alterations in AD and dementia. Findings in literature are in support of such associations, arguing in favor of a “true positive”

effect. For example, AD patients are known to show elevated *APOE* expression in the medial temporal regions that are in turn known to be involved in the pathology of the disease[43, 44, 45]. However, further evaluation using null models that test gene specificity reveals that the observed association is not particularly specific to *APOE*, and can also be observed for nearly 150 other brain-expressed genes in AHBA (corresponding to $z$ = 1.65 for AD, null-brain model). This indicates that while potentially an interesting effect, we cannot provide specificity to *APOE* based on the AHBA data alone.

Similarly, analysis of ASD risk genes initially reveals an interesting association between expression patterns of ASD genes and patterns of brain functional alterations seen in Asperger's syndrome, as shown by both linear regression and the null-spin model. One may be easily tempted to take this effect as a meaningful interaction because Asperger's syndrome is a highly heritable subtype of ASD (Grove et al., 2019) and imaging-genetic associations in ASD have been proposed (Ranlund et al., 2018; Xie et al., 2020). Yet, our analysis using null-random/brain models shows that we cannot claim specificity of this effect to ASD genes, as it can similarly be found also for other random genes not related to ASD. This example again indicates that a false-positive conclusion is possibly made in this type of study and that using null models to test gene specificity is important.

Simulations correlating single-gene expression profiles to brain phenotypes further show that only 5% of the observed linear associations satisfied both spatial and gene specificity. Only less than 3% was reported for simulated phenotypes of geographic brain gradients. Such a small proportion is likely attributable to a high auto-correlation between adjacent brain regions in transcriptomic and phenotypic data, leading to a degree of freedom much smaller than the one applied and thus inflated effects (Fulcher et al., 2020). A second consideration is that the transcriptional profiles of a considerable number of genes (16% of all genes) bear high similarity to multiple geographic gradients in the brain. Examinations of one gene or a few genes within this subset of genes will automatically provide insufficient biological information. Only by testing both the spatial and gene specificity, the reported associations between spatial patterns of gene transcription and imaging-derived phenotypes can be argued to be unbiased due to statistical caveats and limitations.

The discussed null models are presented in a simple web-tool called GAMBA, which can be used to probe the association between transcriptomics and common brain structure/function

phenotypes derived from a wide range of neuroimaging data. GAMBA complements other tools that link genetics and brain functions, tools such as NeuroSynth (Yarkoni et al., 2011) and Brain Annotation Toolbox (Liu et al., 2019) that provide similar platforms to visualize and examine brain maps of gene expression patterns and brain maps, but do not directly provide means to test these effects against multiple null-models.

Several methodological points related to the described transcriptome data have to be considered. First, our examples are based on the rich gene expression data from the AHBA (Hawrylycz et al., 2012). Further extensions to other datasets of brain gene expressions, such as PsychENCODE (Wang et al., 2018) and BrainSpan (Johnson et al., 2009) can be easily made (Wei et al., 2019a). Second, we need to consider that AHBA gene expression data is extracted from the post-mortem brains of healthy individuals, i.e. ones with no psychiatric and neurologic conditions. Therefore, results regarding spatial brain patterns of disorders should be interpreted in the context of gene expression of risk genes in brain regions to be a potential marker for a higher susceptibility of these regions in relevant disorders (Romme et al., 2017; McColgan et al., 2018).

In summary, we highlight the need of using null models to investigate both spatial and gene specificity when examining associations between the spatial patterns of gene transcriptomic profiles and imaging-derived brain features.

## Methods

*AHBA gene expression data*

Microarray gene expression data were obtained from the extensive Allen Human Brain Atlas (http://human.brain-map.org), including highly detailed data from six postmortem brains of donors without any neuropathological or neuropsychiatric conditions. Microarray analyses are described in detail in http://help.brain-map.org/display/humanbrain/Documentation. Brain tissue samples of the left hemisphere were obtained from four donors (466 ± 72.6 samples from H0351.1009, H0351.1012, H0351.1015, and H0351.1016), and 946 and 893 samples covering both hemispheres from the remaining two donors (H0351.2001 and H0351.2002). We included tissue samples of cortical and subcortical regions of the left hemisphere and used the expression of 58,692 probes for each brain donor(Romme et al., 2017; Wei et al., 2019a).

We performed probe-to-gene re-annotation using the BioMart data-mining tool (https://www.ensembl.org/biomart/)(Arnatkevičiūtė et al., 2019). Outdated gene symbols were updated and alias gene symbols were replaced by symbols obtained from the HUGO Gene Nomenclature Committee (HGNC) database (http://biomart.genenames.org/), resulting in the inclusion of 20,949 genes. Expression levels that were not well-above background were set to *NaN*. Per donor, and per tissue sample, expression levels of probes annotated to the same gene symbol were averaged, followed by log2-transformation with pseudocount 1. Tissue samples were spatially mapped to FreeSurfer cortical and subcortical regions to obtain region-wise gene expression profiles(French and Paus, 2015). A cortical parcellation of 114 regions (57 per hemisphere) and subcortical segmentation of 7 regions based on the Desikan-Killiany atlas (DK-114) were obtained for the Montreal Neurological Institute (MNI) 152 template using FreeSurfer(Desikan et al., 2006; Fonov et al., 2011; Cammoun et al., 2012). Brain tissue samples were annotated to cortical regions in the DK-114 atlas based on MNI coordinates, computing the nearest gray matter voxel within the MNI ICBM152 template in the FreeSurfer space. Tissue samples with a distance less than 2mm to the nearest gray matter voxel were included. Gene expression profiles of tissue samples belonging to the same cortical region were averaged, resulting in a 6 × 64 × 20,949 data matrix (i.e., donors × brain regions × genes). Within each donor, gene expression per gene was normalized to *z*-scores across all cortical and subcortical regions. Normalized gene expression profiles were averaged across the six donors obtaining a group-level gene expression matrix of size 64 × 20,949. Considering that most neuroimaging data as described in the following sections only include cortical regions, only the cortical expression pattern of each gene (i.e., 57 × 20,949 gene expression matrix) was correlated to the patterns of various neuroimaging findings.

*Neuroimaging phenotypic data*

Connectome metrics used in *example 1* were obtained from a human structural connectome map reconstructed using T1-weighted and diffusion-weighted MRI (dMRI) data of 487 subjects (age [mean ± standard deviation]: 29.8 ± 3.4 years old) from the Human Connectome Project(Van Essen et al., 2013). Disease maps used *in example 2* and *example 3* were computed based on coordinate-based results obtained from the extensive BrainMap database (http://www.brainmap.org/) that contains published functional and structural neuroimaging experiments of psychiatric and neurological disorders (see Supplementary Methods for a detailed description of the used procedures).

*Statistics and null models*

*Linear regression.* Linear regression is used to test for an association between the cortical expression profile of a gene (or the average expression pattern across a set of genes) and the pattern of an imaging-derived brain phenotype:

$$Y_i = \beta_0 + \beta_1 X_j + \varepsilon \qquad (1)$$

where $Y_i$ indicates the standardized gene expression profile of gene $i$ or the standardized, averaged profile of a gene set $i$, and $X_j$ the standardized cortical profile of neuroimaging phenotype $j$. Standardization is performed by dividing each value $X$ or $Y$ by the standard deviation. The standardized regression coefficient $\beta_1$ and the corresponding correlation coefficient and $p$-value are obtained.

*Null-spin model.* An important variant on the linear regression model was recently introduced(Alexander-Bloch et al., 2018), now testing whether the observed association is specific to spatial-anatomical relationships between brain regions. To this end, in (1) the observed $\beta_1$ is compared to $\beta_1$s generated by 1,000 permutations, in which the gene expression data matrix is rebuilt using randomized brain parcellations by spinning the reconstructed sphere of the real brain parcellation with random angles (0-360°) conserving the spatial relationship of neighboring regions.

*Null-random model.* The null-random model tests whether the observed association is specific to the given gene or set of genes of interest (GOI), i.e. comparing against effects that can be observed when any other set of genes would have been selected. To this end, it is tested whether the observed $\beta_1$ (i.e., the effect size) is different from null distributions of $\beta_1$ observed for randomly selected genes with the null-random distribution estimated from 10,000 permutations and the mean ($\mu$) and standard deviation ($\sigma$) of *effect sizes* in the null distribution obtained.

*Null-coexpression model.* The null-coexpression model includes a stricter null model where random genes with similar co-expression levels as the given GOI are selected to generate null distributions of $\beta_1$ (null-coexpression model). Random genes are selected according to the following steps: first, a set of random genes are initially selected. Then the mean co-expression level of the random gene set is compared to the mean co-expression level of the given GOI. If the co-expression difference is larger than the maximum difference

allowed, the gene with the highest/lowest co-expression level is excluded and a new random gene is included in the set. This step repeats until the co-expression difference is smaller than the maximum difference allowed. A total number of 1,000 sets of random genes were obtained due to the limitation of computational capacity.

*Null-brain model.* The null-brain model is generated using random genes selected from a pool of 2957 genes specially over-expressed in brain tissue, with brain-expressed genes identified by performing one-tail two-sample t-tests on gene expression levels between brain tissues and other body sites ($q < 0.05$, FDR corrected), using gene expression data from the GTEx portal (https://www.gtexportal.org). Permutation is performed 10,000 times.

For all null models, the mean ($\mu$) and standard deviation ($\sigma$) of effect sizes ($\beta_1$) in the null distributions are estimated. A two-tailed $z$-test is performed to examine whether the observed $\beta_1$ (i.e., the effect size) is larger than the mean effect size derived from null models:

$$z = \frac{\beta_1 - \mu}{\sigma}$$

where $\mu$, $\sigma$ indicate the mean and standard deviation of $\beta_1$ over random permutations. A two-tailed $p$-value is computed as follows:

$$p = 2\Phi(|-z|)$$

where $\Phi$ is the standard normal cumulative distribution function.

**Data availability**

Human gene expression data is available in the Allen Brain Atlas ("Complete normalized microarray datasets", http://human.brain-map.org). The GTEx data used is available in the GTEx Portal ("The median RPKM by tissue", https://www.gtexportal.org). The human MRI data (used for the connectome reconstruction) that support the findings of this study are available from the Human Connectome Project (https://www.humanconnectome.org). BrainMap data that support the findings of this study are available at http://www.brainmap.org/.

**Declarations of interest**

none

**Acknowledgments**

The work of M.P.v.d.H. was supported by an ALW open (ALWOP.179) and VIDI (452-16-015) grant from the Netherlands Organization for Scientific Research (NWO) and a Fellowship of MQ. D.P. was supported by The Netherlands Organization for Scientific Research (NWO VICI 453-14-005). S.C.d.L. was supported by the Amsterdam Neuroscience alliance grant. Human neuroimaging data was kindly provided by the Human Connectome Project, WU-Minn Consortium (Principal Investigators: David Van Essen and Kamil Ugurbil; 1U54MH091657) funded by the 16 NIH Institutes and Centers that support the NIH Blueprint for Neuroscience Research; and by the McDonnell Center for Systems Neuroscience at Washington University.

**References**

Alexander-Bloch AF, Shou HC, Liu SY, Satterthwaite TD, Glahn DC, Shinohara RT, Vandekar SN, Raznahan A (2018) On testing for spatial correspondence between maps of human brain structure and function. Neuroimage 178:540–551.

Anderson KM, Collins MA, Kong R, Fang K, Li J, He T, Chekroud AM, Yeo BTT, Holmes AJ (2020) Convergent molecular, cellular, and cortical neuroimaging signatures of major depressive disorder. Proc Natl Acad Sci U S A 117:25138–25149.

Arnatkevičiūtė A, Fulcher BD, Fornito A (2019) A practical guide to linking brain-wide gene expression and neuroimaging data. Neuroimage.

Burt JB, Demirtaş M, Eckner WJ, Navejar NM, Ji JL, Martin WJ, Bernacchia A, Anticevic A, Murray JD (2018) Hierarchy of transcriptomic specialization across human cortex captured by structural neuroimaging topography. Nat Neurosci 21:1251–1259.

Callahan BL, Bierstone D, Stuss DT, Black SE (2017) Adult ADHD: Risk Factor for Dementia or Phenotypic Mimic? Front Aging Neurosci 9:260.

Cammoun L, Gigandet X, Meskaldji D, Thiran JP, Sporns O, Do KQ, Maeder P, Meuli R, Hagmann P (2012) Mapping the human connectome at multiple scales with diffusion spectrum MRI. J Neurosci Methods 203:386–397.

Consortium, G. TEx (2015) Human genomics. The Genotype-Tissue Expression (GTEx) pilot analysis: multitissue gene regulation in humans. Science 348:648–660.

de Lange SC et al. (2019) Shared vulnerability for connectome alterations across psychiatric and neurological brain disorders. Nature Human Behaviour 3:988–998.

de Leeuw CA, Stringer S, Dekkers IA, Heskes T, Posthuma D (2018) Conditional and interaction gene-set analysis reveals novel functional pathways for blood pressure. Nat Commun 9:3768.

Desikan RS, Ségonne F, Fischl B, Quinn BT, Dickerson BC, Blacker D, Buckner RL, Dale AM, Maguire RP, Hyman BT, Albert MS, Killiany RJ (2006) An automated labeling system for subdividing the human cerebral cortex on MRI scans into gyral based regions of interest. Neuroimage 31:968–980.

Fonov V, Evans AC, Botteron K, Almli CR, McKinstry RC, Collins DL, Brain Development Cooperative, Group (2011) Unbiased average age-appropriate atlases for pediatric studies. Neuroimage 54:313–327.

Fornito A, Arnatkeviciute A, Fulcher B (2019) Bridging the Gap between Connectome and Transcriptome. Trends Cogn Sci 23:34–50.

Fox PT, Laird AR, Fox SP, Fox PM, Uecker AM, Crank M, Koenig SF, Lancaster JL (2005) BrainMap taxonomy of experimental design: description and evaluation. Hum Brain Mapp 25:185–198.

Fox PT, Lancaster JL (2002) Opinion: Mapping context and content: the BrainMap model. Nat Rev Neurosci 3:319–321.

Freeze B, Pandya S, Zeighami Y, Raj A (2019) Regional transcriptional architecture of Parkinson's disease pathogenesis and network spread. Brain 142:3072–3085.

French L, Paus T (2015) A FreeSurfer view of the cortical transcriptome generated from the Allen Human Brain Atlas. Front Neurosci 9:323.

Fulcher BD, Arnatkevičiūtė A, Fornito A (2020) Overcoming bias in gene-set enrichment analyses of brain-wide transcriptomic data. BioRxiv 2020.04.24.058958.

Grothe MJ, Sepulcre J, Gonzalez-Escamilla G, Jelistratova I, Schöll M, Hansson O, Teipel SJ, Alzheimer's Disease Neuroimaging Initiative (2018) Molecular properties underlying regional vulnerability to Alzheimer's disease pathology. Brain 141:2755–2771.

Grove J et al. (2019) Identification of common genetic risk variants for autism spectrum disorder. Nat Genet 51:431–444.

Hawrylycz MJ et al. (2012) An anatomically comprehensive atlas of the adult human brain transcriptome. Nature 489:391–399.

Jansen IE et al. (2019) Genome-wide meta-analysis identifies new loci and functional pathways influencing Alzheimer's disease risk. Nat Genet 51:404–413.

Jansen PR, Nagel M, Watanabe K, Wei Y, Savage JE, de Leeuw CA, van den Heuvel MP, van der Sluis S, Posthuma D (2020) Genome-wide meta-analysis of brain volume identifies genomic loci and genes shared with intelligence. Nat Commun 11:5606.

Johnson MB, Kawasawa YI, Mason CE, Krsnik Ž, Coppola G, Bogdanović D, Geschwind DH, Mane SM, State, Matthew W., Šestan N (2009) Functional and Evolutionary Insights into Human Brain Development through Global Transcriptome Analysis. Neuron 62:494–509.

Kepecs A, Fishell G (2014) Interneuron cell types are fit to function. Nature 505:318–326.

Krienen FM, Yeo BT, Ge T, Buckner RL, Sherwood CC (2016) Transcriptional profiles of supragranular-enriched genes associate with corticocortical network architecture in the human brain. Proc Natl Acad Sci U S A 113:E469–E478.

Laird AR, Lancaster JL, Fox PT (2005) BrainMap: the social evolution of a human brain mapping database. Neuroinformatics 3:65–78.

Liu CC, Liu CC, Kanekiyo T, Xu H, Bu G (2013) Apolipoprotein E and Alzheimer disease: risk, mechanisms and therapy. Nat Rev Neurol 9:106–118.

Liu Z, Rolls ET, Liu Z, Zhang K, Yang M, Du J, Gong W, Cheng W, Dai F, Wang H, Ugurbil K,

Zhang J, Feng J, Wren J (2019) Brain annotation toolbox: exploring the functional and genetic associations of neuroimaging results. Bioinformatics 35:3771–3778.

McColgan P, Gregory S, Seunarine KK, Razi A, Papoutsi M, Johnson E, Durr A, Roos RAC, Leavitt BR, Holmans P, Scahill RI, Clark CA, Rees G, Tabrizi SJ, Track-On, H. D. Investigators (2018) Brain Regions Showing White Matter Loss in Huntington's Disease Are Enriched for Synaptic and Metabolic Genes. Biol Psychiatry 83:456–465.

Ranlund S, Rosa MJ, de Jong S, Cole JH, Kyriakopoulos M, Fu CHY, Mehta MA, Dima D (2018) Associations between polygenic risk scores for four psychiatric illnesses and brain structure using multivariate pattern recognition. NeuroImage: Clinical 20:1026–1036.

Richiardi J et al. (2015) BRAIN NETWORKS. Correlated gene expression supports synchronous activity in brain networks. Science 348:1241–1244.

Romero-Garcia R, Warrier V, Bullmore ET, Baron-Cohen S, Bethlehem RAI (2018a) Synaptic and transcriptionally downregulated genes are associated with cortical thickness differences in autism. Mol Psychiatry.

Romero-Garcia R, Whitaker KJ, Vasa F, Seidlitz J, Shinn M, Fonagy P, Dolan RJ, Jones PB, Goodyer IM, Consortium, Nspn, Bullmore ET, Vertes PE (2018b) Structural covariance networks are coupled to expression of genes enriched in supragranular layers of the human cortex. Neuroimage 171:256–267.

Romme IA, de Reus MA, Ophoff RA, Kahn RS, van den Heuvel MP (2017) Connectome Disconnectivity and Cortical Gene Expression in Patients With Schizophrenia. Biol Psychiatry 81:495–502.

Schizophrenia Working Group of the Psychiatric Genomics, Consortium (2014) Biological insights from 108 schizophrenia-associated genetic loci. Nature 511:421–427.

Scholtens LH, van den Heuvel MP (2018) Multimodal connectomics in psychiatry: bridging scales from micro to macro. Biological Psychiatry: Cognitive Neuroscience and Neuroimaging Available at: https://www.sciencedirect.com/science/article/abs/pii/S245190221830096X?via%3Dihub.

Vaishnavi SN, Vlassenko AG, Rundle MM, Snyder AZ, Mintun MA, Raichle ME (2010) Regional aerobic glycolysis in the human brain. Proc Natl Acad Sci U S A 107:17757–17762.

van den Heuvel MP, Scholtens LH, Kahn RS (2019) Multiscale Neuroscience of Psychiatric Disorders. Biol Psychiatry 86:512–522.

van den Heuvel MP, Sporns O (2013) Network hubs in the human brain. Trends Cogn Sci 17:683–696.

Van Essen DC, Smith SM, Barch DM, Behrens TE, Yacoub E, Ugurbil K, Consortium, W. U-Minn HCP (2013) The WU-Minn Human Connectome Project: an overview. Neuroimage 80:62–79.

Vertes PE, Rittman T, Whitaker KJ, Romero-Garcia R, Vasa F, Kitzbichler MG, Wagstyl K, Fonagy P, Dolan RJ, Jones PB, Goodyer IM, Consortium, Nspn, Bullmore ET (2016) Gene transcription profiles associated with inter-modular hubs and connection distance in human functional magnetic resonance imaging networks. Philos Trans R Soc Lond B Biol Sci 371.

Vogel JW, La Joie R, Grothe MJ, Diaz-Papkovich A, Doyle A, Vachon-Presseau E, Lepage C, Vos de Wael R, Thomas RA, Iturria-Medina Y, Bernhardt B, Rabinovici GD, Evans AC (2020) A molecular gradient along the longitudinal axis of the human hippocampus informs large-scale

behavioral systems. Nat Commun 11:960.

Wang D et al. (2018) Comprehensive functional genomic resource and integrative model for the human brain. Science 362 Available at: https://www.ncbi.nlm.nih.gov/pubmed/30545857.

Wang GZ, Belgard TG, Mao D, Chen L, Berto S, Preuss TM, Lu HZ, Geschwind DH, Konopka G (2015a) Correspondence between Resting-State Activity and Brain Gene Expression. Neuron 88:659–666.

Wang Z, Dai Z, Gong G, Zhou C, He Y (2015b) Understanding structural-functional relationships in the human brain: a large-scale network perspective. Neuroscientist 21:290–305.

Wei Y, de Lange SC, Scholtens LH, Watanabe K, Ardesch DJ, Jansen PR, Savage JE, Li L, Preuss TM, Rilling JK, Posthuma D, van den Heuvel MP (2019a) Genetic mapping and evolutionary analysis of human-expanded cognitive networks. Nat Commun 10.

Wei Y, Scholtens LH, Turk E, van den Heuvel MP (2019b) Multiscale examination of cytoarchitectonic similarity and human brain connectivity. Network Neuroscience 3:124–137.

Xie Y, Zhang X, Liu F, Qin W, Fu J, Xue K, Yu C (2020) Brain mRNA Expression Associated with Cortical Volume Alterations in Autism Spectrum Disorder. Cell Rep 32:108137.

Yarkoni T, Poldrack RA, Nichols TE, Van Essen DC, Wager TD (2011) Large-scale automated synthesis of human functional neuroimaging data. Nat Methods 8:665–U95.

Yeo BT, Krienen FM, Eickhoff SB, Yaakub SN, Fox PT, Buckner RL, Asplund CL, Chee MW (2016) Functional Specialization and Flexibility in Human Association Cortex. Cereb Cortex 26:465.

Yeo BT, Krienen FM, Sepulcre J, Sabuncu MR, Lashkari D, Hollinshead M, Roffman JL, Smoller JW, Zollei L, Polimeni JR, Fischl B, Liu H, Buckner RL (2011) The organization of the human cerebral cortex estimated by intrinsic functional connectivity. J Neurophysiol 106:1125–1165.

Zeng H et al. (2012) Large-scale cellular-resolution gene profiling in human neocortex reveals species-specific molecular signatures. Cell 149:483–496.